Research Article

Stepping Stones in CO₂ Utilization: Optimizing the Formate to Oxalate Coupling Reaction Using Response Surface Modeling

Eric Schuler, Marit Stoop, N. Raveendran Shiju, and Gert-Jan M. Gruter*

Cite This: *ACS Sustainable Chem. Eng.* 2021, 9, 14777−14788

Read Online

| ACCESS | | Metrics & More | | Article Recommendations | | Supporting Information |

ABSTRACT: One of the crucial steps for the conversion of CO_2 into polymers is the catalytic formate to oxalate coupling reaction (FOCR). Formate can be obtained from the (electro)catalytic reduction of CO_2, while oxalate can be further processed toward building blocks for modern plastics. In its 175 year history, multiple parameters for the FOCR have been suggested to be of importance. Yet, no comprehensive understanding considering all those parameters is available. Hence, we aim to assess the relative impact of all those parameters and deduce the optimal reaction conditions for the FOCR. We follow a systematic two-stage approach in which we first evaluate the most suitable categorical variables of catalyst, potential poisons, and reaction atmospheres. In the second stage, we evaluate the impact of the continuous variables temperature, reaction time, catalyst loading, and active gas removal within previously proposed ranges, using a response surface modeling methodology. We found KOH to be the most suitable catalyst, and it allows yields of up to 93%. Water was found to be the strongest poison, and its efficient removal increased oxalate yields by 35%. The most promising reaction atmosphere is hydrogen, with the added benefit of being equal to the gas produced in the reaction. The temperature has the highest impact on the reaction, followed by reaction time and purge rates. We found no significant impact of catalyst loading on the reaction within the ranges reported previously. This research provides a clear and concise multiparameter optimization of the FOCR and provides insight into the reaction cascade involving the formation and decomposition of oxalates from formate.

KEYWORDS: CO_2 utilization, Oxalate production, Formate to oxalate coupling reaction, Design of experiments, DoE, Response surface modeling, RSM
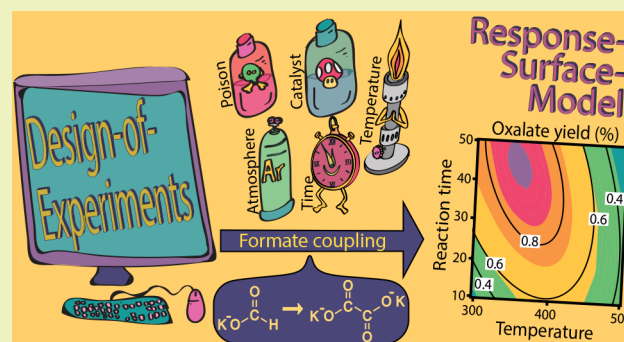
INTRODUCTION

The coupling of formate molecules to oxalate was an important commercial source once for the production of multicarbon compounds until the advent of petrochemical routes.[1−3] The reaction consists of the C−C coupling of two alkali metal formate molecules to form oxalate and hydrogen. Today we are searching for ways to reduce CO_2 emissions and atmospheric CO_2 concentrations to prevent adverse effects on our ecosystems.[4−8] Using CO_2 as an industrial feedstock has the added benefits of low or even negative cost and high abundance.[9−11] Carbon capture and utilization processes are most suitable to live up to this task and are widely developed by academia and industry.[7,8,12−20] With the advent of new routes of sustainable carbon compounds starting from CO_2, formate coupling is increasingly important. One example is the European Horizon 2020 project "OCEAN" in which we develop a continuous process from CO_2 to polymers.[21] In Figure 1 the full reaction cascade of the OCEAN project is shown: In the first step, CO_2 undergoes electrochemical conversion to formate salt. Our research focuses on the electrochemical reduction of CO_2 to formate and to CO, both
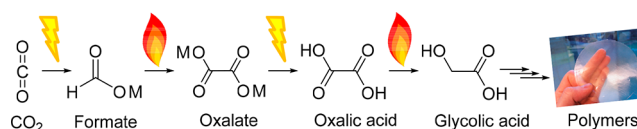

Figure 1. OCEAN process for CO_2 utilization via (i) electrochemical reduction to formate, (ii) thermal formate coupling to oxalate, (iii) electrochemical oxalate acidification, (iv) thermocatalytic reduction of oxalic acid to glycolic acid, and (v) polymer production from oxalic acid and its derivatives.

of which do not require hydrogen and elevated temperatures.[22,23] As formate and CO can both be obtained via a two-electron electrochemical reduction of CO_2, the electrochemical

production of formate from CO_2 aligns well with the ambition to use CO_2 as a renewable C1 feedstock.[24,25] The formate can be effectively recovered from the solution by a combination of evaporation and cooling crystallization. In the second step, these formates are catalytically coupled to oxalate in the formate coupling reaction (FOCR), which is the subject of this paper. Formate is then acidified to oxalic acid in the third step. The fourth step of the technology targets the derivatization of oxalic acid to esters or its conversion to produce monomers such as glycolic acid. In the fifth (and final) step, we investigate new high-performing polymers from these CO_2-based monomers.[26−29] Polymers can be especially interesting as they allow for long-term storage of sequestered CO_2 in materials.[9,10] CO_2-based chemicals such as oxalic acid will become new platform chemicals for a wide range of downstream products such as monoethylene glycol (MEG), glycolic acid, and glyoxylic acid that all can be obtained from oxalic acid in various sustainable routes.[26,30]

The formate to oxalate coupling reaction (FOCR) is influenced by many factors and has been intensively studied since the 19th century for industrial and scientific interests. From the beginning of the 20th century until the 1930s, nine patents were published about the reactor and the reaction conditions for industrial use.[31−40] The reaction kinetics and the process optimization were studied extensively by Freidlin between 1937 and 1941, resulting in at least 14 publications covering this particular reaction.[41−52] The different gaseous and solid products from thermal decomposition of formate have been studied by Shishido and Górski in the period 1970−1990.[53−58] In the past 10 years, interest has sparked with new patents and studies on new reactor configurations and novel mechanistic studies.[59−66] Most recently, we showed that using superbases as catalysts can dramatically reduce the required reaction temperature and time while simultaneously increasing the oxalate yield.[65]

The desired reaction in the FOCR is the formation of oxalate and hydrogen from two formate molecules (eq 1).

$$2HCOOK_{(s,l)} \xrightarrow{\triangle} K_2C_2O_{4(s)} + H_{2(g)} \tag{1}$$
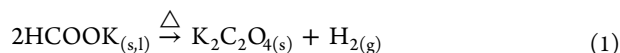
Formates are salts of formic acid with metals as counterions, such as alkali, transition, and second-row metals. The formate decomposition temperature and resulting products depend on their metal counterion. All formate salts decompose at high temperatures above 450 °C to carbonates, metal oxides, or metals but only rarely to the desired oxalate. Only alkali metal formates favor the formation of oxalate. Sodium and potassium formates are most commonly used for the FOCR. They give higher oxalate yields at lower temperatures in comparison to lithium, rubidium, and cesium formates. The main side product in the FOCR is the formation of carbonate, which was suggested to be derived from formate directly (eq 2) or by the subsequent decomposition of oxalate (eq 3).

$$2HCOOK_{(s,l)} \rightarrow K_2CO_{3(s)} + CO_{(g)} + H_{2(g)} \tag{2}$$

$$K_2C_2O_{4(g)} \rightarrow K_2CO_{3(s)} + CO_{(g)} \tag{3}$$
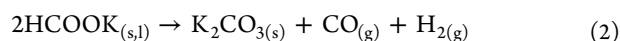
Several different reaction mechanisms have been suggested for the formate coupling reactions over the years and are discussed in detail in our recent perspective ar-

ticle.[44,56,58,64,67−69] The reaction is catalyzed by bases, which increase the likeliness of the formation of the carbonite intermediate which is crucial for the coupling reaction to occur.[46,47] The stronger the base, the higher its capability to abstract the proton from the formate, which initiates the reaction, allowing operation at lower temperature and resulting in higher selectivity.[64]

However, the basicity of the catalyst is not the only parameter that influences the reaction. To improve the industrial process of oxalate production, it is essential to know and understand the ideal reaction conditions and parameters for the FOCR. During our studies, we have identified several factors. However, the reported values for the optimized parameters differ significantly depending on the used reactor configuration and often contradict another, both in optimal values and even in the nature of influence: positive or negative. In our recent perspective paper, we provide a comprehensive overview and discussion of previously proposed factors influencing the formation of oxalates from metal formates as shown in Figure 2.[69] To this day, no systematic approach has been used to comprehensively investigate these parameters as well as their interdependency. In this research, we aim to provide a complete overview of potential factors reported in previous literature, and we will estimate their importance and interdependency. As this work is part of the OCEAN project, we only tested reaction parameters for potassium formate due to its suitability as a counterion in the electrochemical conversion process of CO_2 to formate.[29]

As we will focus on potassium formate, being the product produced in the electrocatalytic CO_2 reduction, we explore the remaining five pillars from Figure 2: heating, atmosphere, catalysts, poisons, and reaction time. These groups contain categorial factors such as atmosphere or choice of catalyst and continuous numerical factors such as temperature or reaction time. Previously, several parameters were systematically evaluated, but in other instances, these were just resulting from the reactor designs or the purities of the used reactants. Reaction temperatures and times fall in the first category, and these have been tested deliberately while the flow rate of gas, or the absence thereof, was mostly a result of the experimental setup and reactor design. Our goal is therefore to create a comprehensive understanding of the impact and optimal values of each parameter as well as to uncover interactions between them. We focus hereby on factors that were reported to lead to the formation of oxalate and are relevant today. This led to the exclusion of poisonous and dangerous catalyst systems such as alkali metal amalgams or expensive and scarce platinum as the reactor material of construction. While we cover the full range of previously reported reaction temperatures, catalyst loadings, and a wide range of purge flows, we restricted ourselves to reaction times up to 60 min. The main reason for this is the undesirability of long reaction times for continuous reactor designs.

■ RESULTS AND DISCUSSION

We approach this evaluation in two stages as illustrated in Figure 3. First, we identify the impact of categorical factors and identify the best catalyst, potential poisons, and most suitable atmosphere. In the second stage, we evaluate the impact and ideal range of the numerical factors using design of experiments (DoE) and a response surface model (RSM).[70] To be able to test all the parameters reported previously, we
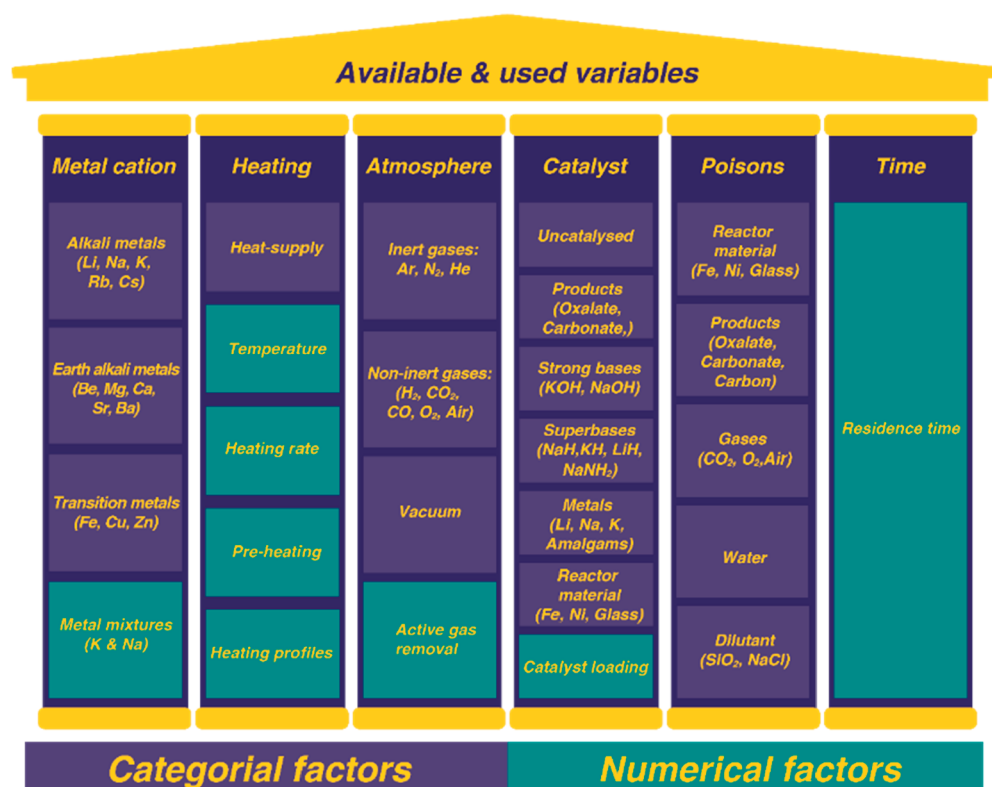
Figure 2. Parameters available and historically investigated for the FOCR, categorized in six pillars including the metal cation of formate, heating of the reaction, reaction atmosphere, catalyst choice, potential poisons, and reaction time.
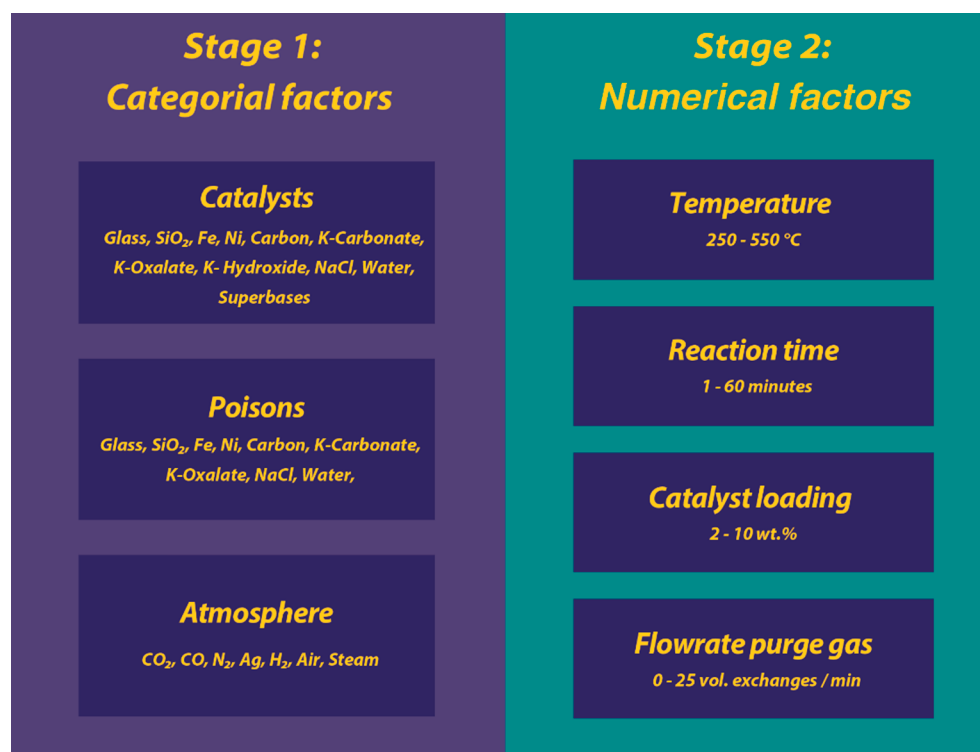

Figure 3. Two-stage approach to systematically assess the impact of factors relevant in the FOCR. In stage 1, categorial factors such as catalysts, poisons, and atmospheres are tested for their suitability and potential impact. The best suitable combinations are then carried over to stage 2, in which response surface models are created to identify the individual impact, interactions, and optimal values for each of the factors within the ranges used before in the literature.

purposely developed a reactor system that allowed for the deliberate variation of all factors within the proposed ranges.

Catalyst. In the 175 year history of the FOCR, different catalysts were proposed in the literature, and we tested them under identical conditions. We did not include superbases and alkali metals as we have tested them successfully, which was reported in another publication.[65] Each test was performed in duplicate and in random order to ensure statistically relevant results. For each catalyst, 5 wt % loading was used to convert potassium formate in a nitrogen atmosphere with a flow of 25 mL/min (corresponding to 3.5 reactor volume exchanges/min) at a temperature of 400 °C for 8 min. With potassium hydroxide, we achieved by far the highest oxalate yield as shown in Figure 4A. The oxalate yield without any catalyst is below 2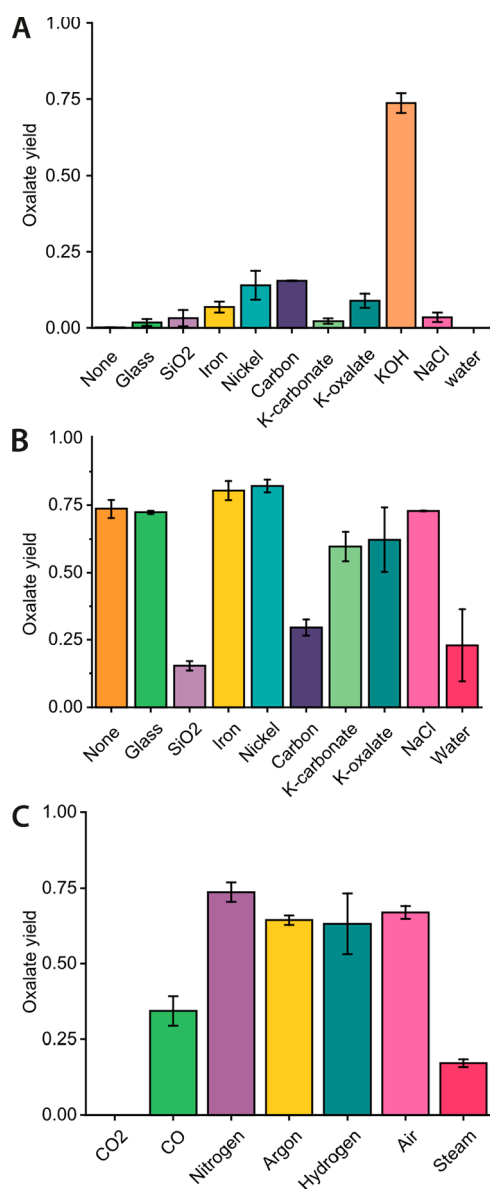0% due to an overall low conversion at this temperature and reaction time. In our previous work, we have shown that in the absence of catalyst higher temperatures of up to 420−440 °C and longer reaction times of 150−200 min are required, yet only marginal yield gains up to 21% oxalate yield could be achieved as carbonate formation is favored at higher temperatures.[65] The carbon balance, conversion, and selectivity are shown in Figure S2. For the other potential catalysts (glass, SiO_2, iron, nickel, carbon, potassium carbonate, potassium oxalate, and NaCl), the conversion of formate is low. The selectivity toward oxalate is below 50% for all of them, leading to oxalate yields below 20%, and we, therefore, conclude that they do not act as catalysts. Water also does not act as a catalyst and even entirely stops the FOCR. We introduced water in two ways: as liquid added to the reaction mixture before heating and as steam added to the nitrogen stream during the reaction. As a result of both ways of water introduction, formate is converted mainly to carbonate. The low carbon balance indicates further reaction toward gaseous products as no undissolved solids were observed. Among the proposed catalysts, KOH is the most suitable catalyst for the FOCR. KOH as a catalyst favors high conversion with 89% selectivity toward oxalate. Hence, we decided to use KOH as a catalyst for the remaining tests.

Strictly speaking, KOH is not acting as a catalyst itself. We recently proposed that hydride is the active species that is formed in situ in an equilibrium reaction from hydroxide.[69,71] We could prove this with high-resolution kinetic studies and molecular dynamics calculations. The equilibrium can be shifted toward the formation of hydride with the removal of water from the reaction. The full reaction cycle, as shown in Scheme 1, therefore starts with the in situ generation of hydride. This then catalyzes the formation of the reactive carbonite intermediate from formate, during which hydrogen is released. This hydride mechanism was first proposed by Lakkaraju et al., and we recently confirmed the important role of carbonite with isotopic labeling studies and molecular dynamics calculations.[64,65] Carbonite then forms oxalate in a nucleophilic attack on another formate. In the last step, hydride is released and catalyzes a subsequent coupling reaction.

Poisons. In the second step, we evaluated the effect of potential poisons on the hydroxide catalyzed FOCR. We restrict ourselves to the poisoning effects on the hydroxide catalyzed reaction as this reaction shows clear benefits over the uncatalyzed reactions. Poisons were reported to affect either the overall formate conversion or the selectivity toward oxalate. Especially the effect of metals used for the reactor material of construction is of interest. The same conditions as in the first design were chosen. All reactions were performed in duplicate and in random order to ensure statistically relevant results. For each reaction, KOH was used as a catalyst with a 5 wt % loading, with respect to the reactant potassium formate. This was done in a nitrogen atmosphere with a flow of 25 mL/min (corresponding to 3.5 reactor volume exchanges/min) at a temperature of 400 °C for 8 min. Each potential poison was added at 5 wt % loading with respect to the reactant formate salt. Water, silica, and carbon significantly influence the oxalate yield as shown in Figure 4B. In Figure S3 we see that the addition of water and dry silica strongly decreases the conversion. The addition of carbon decreases the conversion as well, and the selectivity shifts toward carbonate instead of the targeted oxalate formation. The morphology of carbon and silica could be causing these effects when added as a poison.

Figure 4. Oxalate yields achieved in the categorial tests to evaluate (A) best catalyst at 5 wt % loading, (B) effect of potential poisons at 5 wt % in reactions catalyzed with 5 wt % hydroxide, and (C) different atmospheres in a reaction catalyzed with 5 wt % hydroxide. Temperature, gas flow, and reaction times were kept constant at 400 °C, 10 min, and 3.5 volume exchanges/min for all reactions.

Scheme 1. Hydroxide Catalyzed Formate Coupling via (i) In Situ Hydride Generation, (ii) Carbonite and Hydrogen Formation via Proton Abstraction from Formate by Hydride, and (iii) Oxalate and Hydride Formation via Nucleophilic Attack of Carbonite on Formate and Subsequent Hydride Elimination
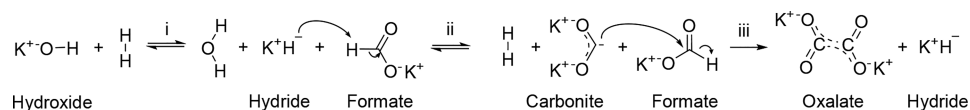
Both are puffy powders and therefore good insulators. The heat supply is most likely hindered and therefore the apparent reaction temperature is decreased, causing a lower conversion. We cannot explain yet the increase in carbonate formation with carbon as the poison. Potassium carbonate and potassium oxalate have a small negative influence on the FOCR with KOH when added as additives before the reaction. The conversion of formate for reactions in which these two compounds were added is similar, but the selectivity toward oxalate decreased slightly. NaCl, glass, iron, and nickel do not influence the selectivity of the FOCR with KOH. For NaCl and glass, the conversion of formate is also not influenced. However, iron and nickel increase the conversion of formate and therefore lead to a higher oxalate yield. The carbon balance is above 93% in all these reactions, and only a small amount of carbon between 2 and 7% is lost during the reaction. Water, silica, and carbon have a poisonous effect on the FOCR. In our view, the strong poisoning effects of water present a special challenge due to the hygroscopic nature of both formate and hydroxide. Formate has gained its new interest today due to new production routes from direct electrochemical reduction of CO_2. As formate is obtained as an aqueous solution in this process, the need for absolute water removal in the FOCR is especially noteworthy.

Suitable Reaction Atmospheres for the FOCR. The production of equimolar amounts of hydrogen in the process is often neglected, yet its harvest might improve the overall process economics. Various atmospheres including carbon dioxide, carbon monoxide, nitrogen, argon, hydrogen, air, and steam have been proposed as suitable for or detrimental to the reaction performance. We tested each atmosphere for its suitability in the hydroxide catalyzed FOCR and performed the tests in duplicate and random order to ensure statistical relevance. For each reaction, KOH was used as a catalyst with a 5 wt % loading to convert potassium formate. The reaction conditions were the same as above (gas flow of 25 mL/min, corresponding to 3.5 reactor volume exchanges/min, at a temperature of 400 °C for 8 min). The highest yield is achieved in nitrogen with high values also achieved in hydrogen, argon, and air (Figure 4C). Conversely, CO_2 prevents conversion almost completely and only carbonate is formed as shown in Figure S4. In carbon monoxide, the conversion is still low at 13% but the selectivity toward oxalate is higher at 83%. This is in line with the observations of Górski et al. for carbon monoxide, yet they did observe oxalate formation at lower levels using CO_2.[56] Water, in gaseous form, again has a negative influence on oxalate yields. We introduced steam by enriching a stream of nitrogen with water vapor. Figure S4C,D reports this decrease in conversion and a shift toward the formation of carbonate compared to using a dry nitrogen atmosphere. Air and hydrogen behave similarly to inert gases, argon, and nitrogen. In contrast to the literature reports, the oxygen in the air did not react with the intermediate. Moisture in the air can lead to the poisoning effects observed in literature rather than the presence of

oxygen. Although the cheapest option, dry air is not desirable in this reaction due to the production of hydrogen, increasing the explosion risks. The complicated separation of hydrogen from gas mixtures for its valorization is another hindering factor. Nitrogen atmospheres lead to the highest conversions at 84%, with high selectivity to oxalate of 89%. Formate conversion in hydrogen atmosphere shows high conversion as well as the highest selectivity toward oxalate and no selectivity to carbonate. During the reaction, hydrogen is produced, and if a hydrogen stream is used in the reaction, downstream separation is not required for its valorization. Overall, nitrogen and hydrogen are the most suitable atmospheres and the gases should be dried before use. In continuous commercial processes, a hydrogen atmosphere is the most desirable, as the use of hydrogen allows for direct utilization of the produced hydrogen without gas separation. Also, no additional gas is needed as the hydrogen purge gas is supplied as a product from the reaction itself. CO_2 is the least favorable atmosphere and together with carbon monoxide can be added to the list of potent poisons for the reaction.

Purging and the Effect of Volume Exchange. To evaluate the influence of purging and to identify the ideal purging rate, a suitable test range is required. The purge gas has two potential functions: either the removal of reaction products to drive equilibrium reactions or the removal of poisons. Water is a reaction product as well as a poison, and its removal is crucial for the in situ generation of the active hydride catalyst in the FOCR. In our experiments where we analyzed the composition of the purge gas from the reactor, we observed a strong increase in reaction activity after the water content in the off-gas had dropped significantly.[71] This is most likely the main benefit of purging. We tested only nitrogen and hydrogen as purge gases due to their suitability as atmospheres in the reaction. We were unable to find conclusive information on the effect of purging rates on the reaction in the literature. Before designing our experiments for the RSM, we therefore first aimed to establish whether the purging rate has any effect and, if so, which range is most suitable. The selected purging rate limits were mainly determined by the available reactor configuration. We kept the remaining reaction conditions constant at 400 °C, 30 min reaction time, and a catalyst loading of 5 wt %.

Figure 5 shows that purging has a positive effect on the oxalate yield which is pronounced specially for lower purging rates. This improvement of oxalate yields coincides with the increase in conversion and the slight decrease of carbonate production with increasing purging. The improvement in oxalate yield levels out in the chosen range, which indicates its sufficiency to estimate the overall effect and importance of purging in the formate coupling reaction. Purging the reaction benefits the oxalate yield with increasing gas flow, but the incremental improvements level off above exchange of the reactor volume higher than once per minute.

Impact of Temperature, Time, Purge Flow, and Catalyst Loading. In the second stage, we built response
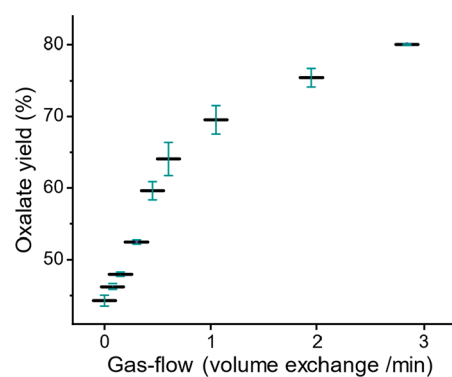
Figure 5. Influence of purging on oxalate yield in formate coupling reaction in a nitrogen atmosphere with 5 wt % potassium hydroxide as a catalyst.

surface models for the most suitable systems established in the first stage. We decided to test two systems that use potassium formate as a reactant and potassium hydroxide as a catalyst, avoid the presence of water, and use either nitrogen or hydrogen as atmosphere. The response surface model is built to assess the impact of temperature, reaction time, catalyst loading, and purge flow speed in two separate response surface models in nitrogen and hydrogen atmospheres. The response surface methodology allows us to cover a large experimental space while keeping the total number of experiments in an acceptable and manageable range. Such modeling approaches have the added benefit that they allow the detection of interactions between parameters and they provide an estimation of a global maximum for the desired responses. We use a central composite design that allows the development of quadratic models including linear, quadratic, and two-factor interaction terms. We performed each experiment in duplicate and performed the experiment for the central point of the design six times. All experiments were performed in totally random order without the use of reactor blocks or reactor arrays. Temperatures (A) were varied from 300 to 500 °C; the details for the other parameters of purging (B), catalyst loading (C), and reaction time (D) are listed in Table 1 for the nitrogen and hydrogen models. Due to equipment limitations, we did not include the purge flow for the model in the hydrogen atmosphere and kept the purge flow constant.

Table 1. Numerical Continuous Factors Used in the RSM with Nitrogen as the Atmosphere

factor	units	min	max
temperature (A)	°C	250	550
purging (B)[a]	volume exchange mL/min	0.15	3.5
catalyst loading (C)	wt %	2.0	10.0
reaction time (D)	min	1.00	60.00

[a]Only used as a variable in the nitrogen response surface model.

As responses, we consider the conversion of formate, oxalate yield, carbonate yield, and the overall carbon balance. We use a coded scale for our regression computations allowing us to interpret and compare the influence of each model term similarly as the reported coefficient estimates are obtained using the same scale.[72]

For the analysis, we first fitted a model with the full quadratic models including linear, two-factor interactions, and quadratic terms. We did not transform the acquired data before the model building. To exclude the presence of higher-order factors and non-Gaussian data distribution, we compared nontransformed model results with a square-root preprocessed model. To improve the model and extract the true influential model parameters, we reduced the model by performing a backward exclusion using the p-value as the discriminating criterion. Only model parameters with a confidence interval higher than 99% or a p-value lower than 0.01 were considered in the reduced model. For our models, we observe an improved overall F-value and better agreement between the calculated and adjusted R^2 values while expectedly reducing the apparent R^2 value due to reduced overfitting by the exclusion of nonsignificant parameters. For the detailed descriptions of the response surface design and statistical relevance of the models, please refer to the Supporting Information.

Our primary goal is to find ideal conditions for high oxalate yields and the individual effects of each tested factor. The obtained oxalate yields for each of the factors in the nitrogen atmosphere are shown in Figure 6, and those for the hydrogen atmosphere are shown in Figure 7. Due to the nature of the central composite design, the values for the three remaining parameters were not kept constant. We see in Figures 6A and 7A, that temperature has the clearest trend of all factors. Oxalate yields first increase until a reaction temperature of 400 °C is reached, after which they decrease. At 400 °C similar oxalate yields are obtained in hydrogen and nitrogen. The average oxalate yield at 300 °C is higher when a hydrogen atmosphere compared to a nitrogen atmosphere is used. However, the yield at temperatures above 400 °C is lower in the hydrogen atmosphere. For the reaction time and purging of the oxalate, yield appears separated in two regimes of lower and higher yields as seen in Figure 6B,D. This indicates the presence of interactions between two factors. In nitrogen, the average oxalate yields appear to be increasing with long reaction times and higher purging rates. In hydrogen, however, the oxalate yield slightly decreases at times longer than 30 min. In both models, the oxalate yields are equally spread throughout the design space for catalyst loading and no effect on the yield is visible from the raw data. The potential presence of interacting factors and nonlinear behavior of oxalate yield justifies the use of a quadratic model to identify the interaction and deconvolute the linear, two-factor-interaction, and quadratic terms. After the deconvolution, the magnitude of the influence of each term can be estimated. Similar trends and analysis for the remaining responses of conversion, carbonate yield, and carbon balance were shown and are explained in detail in the Supporting Information.

Our approach to creating statistically significant models first considers all linear terms, two-factor-interaction terms, and quadratic terms and then eliminate the nonsignificant terms using a strict confidence interval of 99% as a cutoff. For none of the models was catalyst loading found to have any significant influence. In a nitrogen atmosphere, the oxalate yield is significantly influenced by linear terms of temperature, purging, and reaction times. Interactions between temperature and purging as well as the quadratic term of temperature are also significant. The improved reduced model features an R^2 value of 0.907, meaning that 90.7% of the results can be explained by the significant model terms. It is therefore unlikely that another crucial factor was missed out or not controlled. The close resemblance between the adjusted R^2 (0.895) and predicted R^2 (0.880) indicates a high prediction quality of the model.
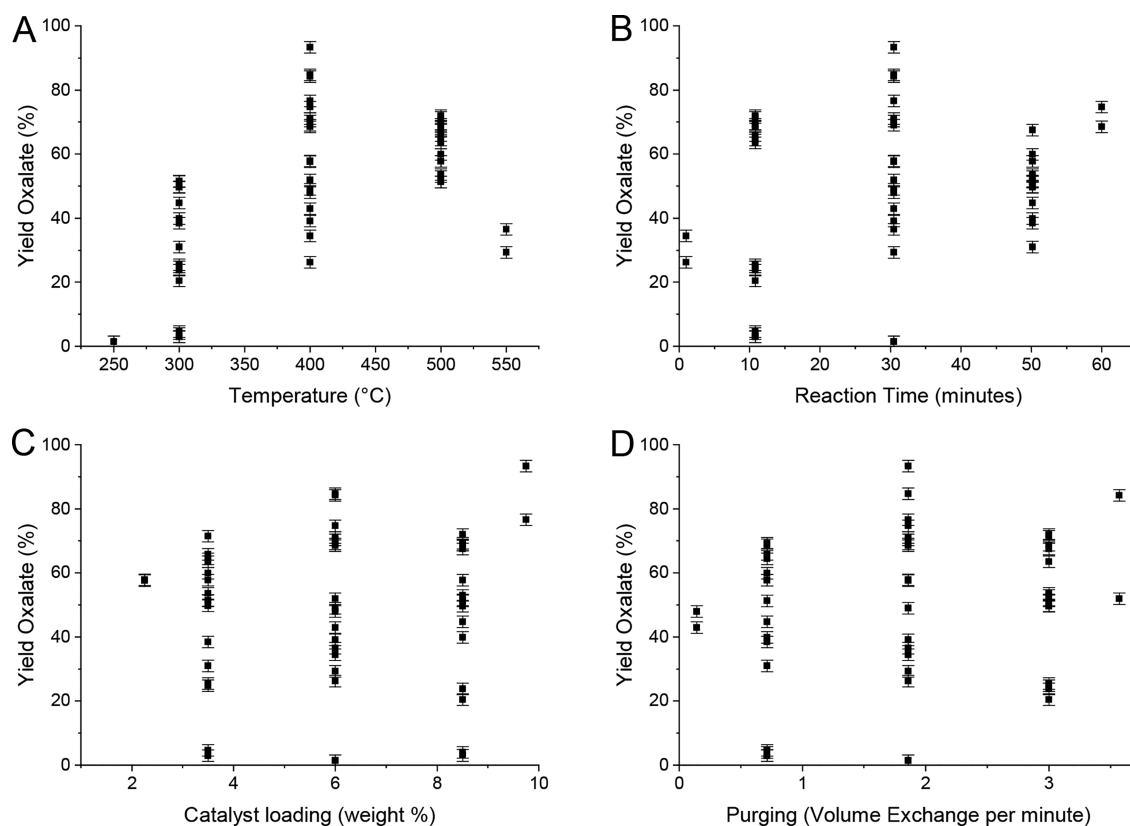
Figure 6. Raw data obtained for oxalate yield in nitrogen atmosphere relative to all four factors: temperature (A), reaction time (B), catalyst loading (C), and purging (D).
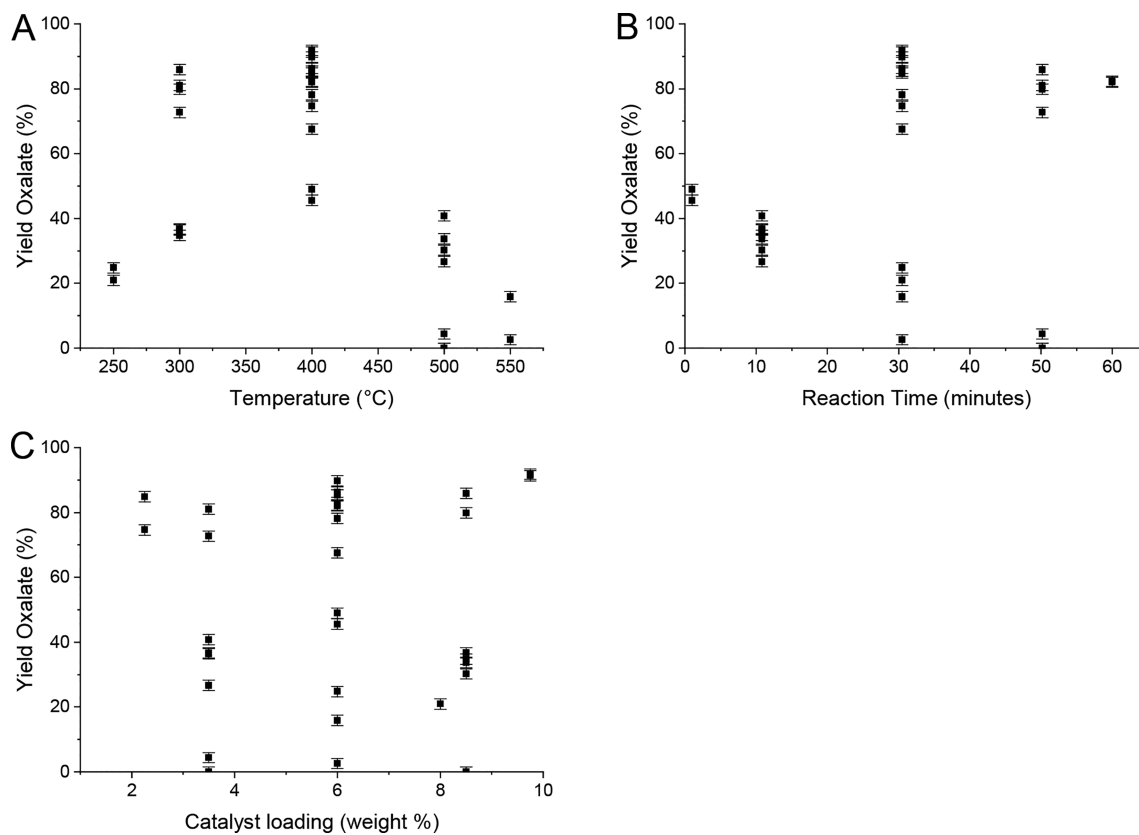

Figure 7. Raw data obtained for oxalate yield in hydrogen atmosphere for all three factors: temperature (A), reaction time (B), and catalyst loading (C).

Table 2. Estimated model moefficients for significant factors describing the model for obtained oxalate zields in a nitrogen atmosphere[a]

factor	coeff est	df	std error	95% CI, low	95% CI, high	VIF
intercept	0.7952	1	0.0152	0.7647	0.8257	
A, temperature	0.1449	1	0.0108	0.1231	0.1666	1.0000
B, purging	0.0492	1	0.0108	0.0274	0.0709	1.0000
D, reaction time	0.0712	1	0.0108	0.0494	0.0929	1.0000
AB	−0.0475	1	0.0122	−0.0721	−0.0229	1.0000
AD	−0.1002	1	0.0122	−0.1248	−0.0756	1.0000
A^2	−0.1697	1	0.0153	−0.2004	−0.1390	1.0000

[a]The intercept is the overall average of all runs, and coefficients are adjusted around that average based on the settings chosen for each factor. The coefficient estimate explains the change in response per unit change in the factor value at constant values for the remaining factors. The variance inflation factor (VIF) is a measure of factor orthogonality where VIF = 1 stands for fully orthogonal factors.

The coefficient estimates listed in Table 2 indicate how much each of the terms affects the oxalate yield. The accumulated effect of terms for each factor is graphically illustrated in Figure 8. Of all significant factors, the linear term
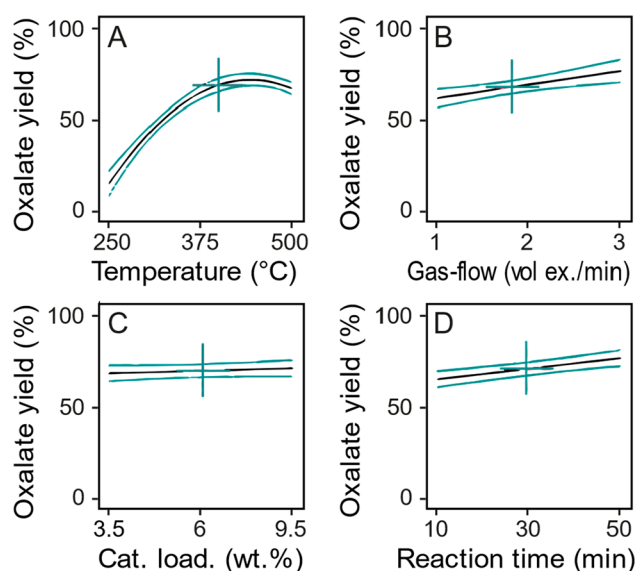

Figure 8. Influence of each factor on oxalate yield of formate at medium values for the remaining factors in the reduced quadratic model. The green bands show the limits of the 95% confidence interval. (A) Temperature shows the highest influence and follows a quadratic term. Higher temperatures favor the oxalate yield until the inflection point at 430 °C. (B) Increasing gas flow linearly increases the oxalate yield. (C) Catalyst loading is no longer considered a contributing factor and is thus a straight line. (D) Oxalate yield linearly increases with longer reaction times.

of temperature has the biggest effect on oxalate yield, but the overall effect of temperature is dampened by its quadratic term and interaction with purging and reaction time. Longer reaction times and higher purging rates benefit the conversion, too. All two-factor interactions and quadratic terms act as dampening terms toward higher values. From a chemical point of view, the increase of oxalate yields with the increase of the factor values makes sense as higher temperatures, longer reaction times, and better removal of side products by purging drive the reaction. Yet, above a certain temperature and with prolonged reaction times the formed oxalate decomposes, which explains the decreasing oxalate yields for high temperatures and reaction times as can be seen from Figure 9B. Our models describing carbonate yields and carbon balances both
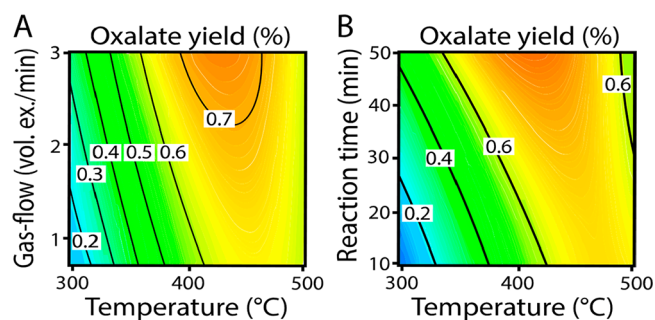

Figure 9. Contour plots for oxalate yields depending on (A) temperature and gas flow and (B) temperature and reaction time with reduced quadratic design.

show increasing carbonate formation (Figure S29) and carbon losses (Figure S33) primarily with increasing temperatures and therefore confirm the strong temperature dependence. The effect of purging increases linearly and positively contributes to oxalate yields. Catalyst loading had no influence on the oxalate yield, conversion, or carbonate formation in the range we tested. This range was based on literature values, and the results indicate that even lower catalyst loadings can be used. In our small-scale reaction setup, we tested lower catalyst loadings; however, they lead to results with error margins too high for response surface modeling. In a commercial process, however, lower loadings should be possible. Yet, if oxalate is acidified in an electrochemical multicompartment acidification cell, then the hydroxide can be fully recovered.[30,73−78] Therefore, an optimization toward very low catalyst loadings would be of lower importance. The lack of benefit of high loadings of hydroxide, the precursor for the in situ generated hydride catalyst, is due to the fact that formate coupling is orders of magnitude faster than the hydride generation.

Overall, the temperature is the main driver for the reactions toward oxalate or carbonate. Oxalate is formed in the whole temperature range, yet above 430 °C a competing reaction toward carbonate or subsequent decomposition of oxalate occurs. Górski reported an increased carbonate formation with higher hydroxide loadings.[56] Our findings contradict theirs and indicate that high reaction temperatures and long residence times are causing oxalate decomposition independent of hydroxide loadings. The decrease in oxalate yield with increasing reaction time at high temperatures above 430 °C (Figure 9A) indicates the presence of a subsequent decomposition reaction. Unfortunately, the model does not present us with a local or global maximum for the oxalate yield as Figure 9 shows. A combination of a lower reaction

temperature with a longer reaction time promises improvements in the achievable oxalate yield in nitrogen atmospheres.

Conversely, in the hydrogen model, we do obtain a local maximum for oxalate yields (Figure 10). Even higher oxalate
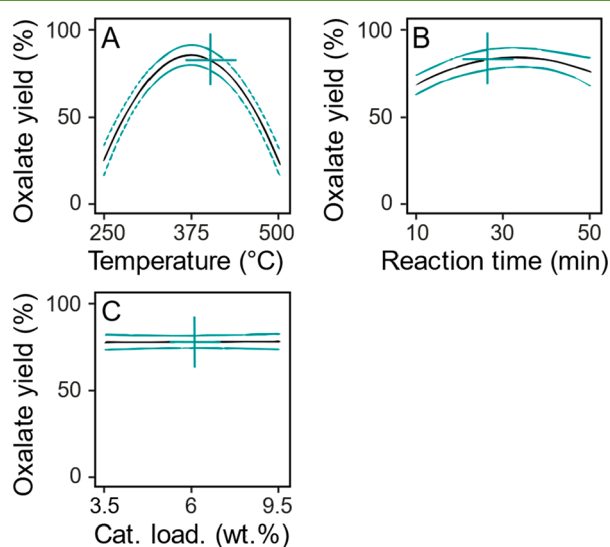

Figure 10. Influence of each factor on oxalate yield at median values for the remaining factors in the reduced quadratic model. The green bands show the limits of the 95% confidence interval. (A) Temperature shows the highest influence and follows a quadratic term with a maximum at 375 °C. (B) Reaction time follows a quadratic term with a maximum at 31 min. (C) Catalyst loading is no longer considered a contributing factor and is thus a straight line.

yields are achieved with temperatures and reaction times compared to the reaction in the nitrogen atmosphere. Our underlying model for oxalate yield in a hydrogen atmosphere is significantly influenced by linear terms of temperature and reaction time, interactions of the latter two, and their quadratic terms. This improved reduced model features an R^2 value of 0.908, meaning that 90.8% of the results can be explained by the significant model terms. The close resemblance between the adjusted R^2 (0.8915) and predicted R^2 (0.8509) indicates a high prediction quality of the model.

The coefficient values for oxalate yields in the hydrogen atmosphere (Table 3) show that the quadratic and linear terms

Table 3. Estimated model Coefficients for Significant Factors Describing the Model for Obtained Oxalate Yields in a Hydrogen Atmosphere[a]

factor	coeff est	std error	95% CI, low	95% CI, high	VIF
intercept	0.8300	0.0333	0.7618	0.8982	
A, temperature	−0.1477	0.0211	−0.1910	−0.1044	1.0000
B, reaction time	0.0611	0.0211	0.0178	0.1044	1.0000
AB	−0.1887	0.0264	−0.2428	−0.1346	1.0000
A^2	−0.3210	0.0252	−0.3727	−0.2694	1.02
B^2	−0.1046	0.0252	−0.1563	−0.0529	1.02

[a]The intercept is the overall average of all runs, and coefficients are adjustments around that average based on the settings chosen for each factor. The coefficient estimate explains the change in response per unit change in the factor value at constant values for the remaining factors. The variance inflation factor (VIF) is a measure of factor orthogonality where VIF = 1 stands for fully orthogonal factors.

of temperature have the biggest effect on oxalate yield. Other than in nitrogen a strong interaction between temperature and reaction time is apparent, and higher temperatures appear to have a stronger negative effect on oxalate yields compared to nitrogen. This can be seen by the magnitude of the coefficient for the quadratic term and in the influence of the factors in Figure 10. The reaction time has a lower effect on the oxalate yield, but a maximum is present within the design space as visible in Figure S10B. Catalyst loading does not affect the oxalate yield. From a chemical point of view, the presence of a maximum oxalate yield makes sense. In the regime leading up to the maximum, the conversion of formate to oxalate is reigning. After the maximum, higher temperatures and longer reaction times lead to the decomposition of the formed oxalate to carbonate. In Figure 11, compared to using a nitrogen
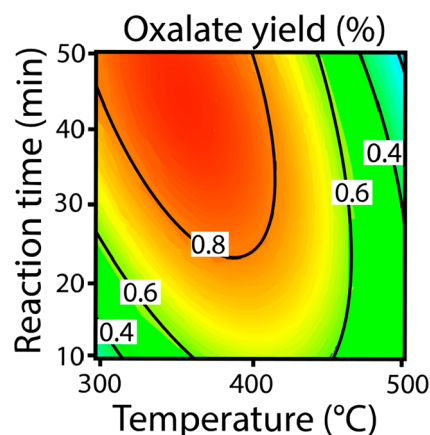

Figure 11. Contour plot for oxalate yields development due to interaction of temperature and reaction time in a hydrogen atmosphere with reduced quadratic design.

atmosphere, high oxalate yields can be achieved at lower reaction temperatures and shorter reaction times. As in a nitrogen atmosphere, the catalyst loading did not influence the oxalate yield, conversion, or carbonate formation in the range we tested. Therefore, even lower catalyst loadings could be realized in practice. Although we tested lower loadings, the results were not consistent enough for RSM. Higher hydroxide loadings did not provide a benefit as the in situ hydride generation is the limiting step for the reaction. The highest oxalate yield was achieved at 355 °C and 45 min reaction time. Furthermore, the term coefficients can be used to find optimal conditions with attribution of importance toward each factor in individual reactor designs.

Overall, in our response surface models temperature, reaction time, and purging have a significant influence on oxalate yields. Catalyst loading does not influence the ranges we chose, which are based on a broad literature search. This indicates that an even lower catalyst loading could be used in the future without any significant drawbacks on reaction performance. This however requires the absence of water, which is challenging due to the hygroscopicity of both hydroxide and formate but also the formation of water in the in situ hydride generation from hydroxide and hydrogen. The positive effect of water removal by active purging confirms this further. Purging is beneficial for the formation of oxalate but does not prevent the formation of carbonate and, therefore, mainly drives conversion without affecting selectivity. While temperature is the dominating factor in nitrogen atmospheres,

reaction time and temperature have more equal effects on oxalate yields in hydrogen. The reaction time influences all four responses and therefore requires control to reach the optimum oxalate formation without leaving the product exposed to high temperatures and risking its decomposition. The comparatively low effect of reaction time on carbonate formation and carbon balance compared to oxalate yield indicates that the relative speeds of decomposition reactions are slower. We propose a linear reaction cascade starting with the formation of oxalate from formate. The oxalate then slowly decomposes to carbonate at high temperatures. At very high temperatures and long reaction times, the carbon is lost from the obtained solids as either nonsoluble elemental carbon or gaseous carbon. There is no more indication of formate decomposition to carbonate at temperatures below 350 °C as suggested previously. We observed very low carbonate yields at low temperatures and no involvement of hydroxide in carbonate formation as the carbonate yield is independent of increasing catalyst loadings.

CONCLUSIONS

In this study, we systematically evaluate the importance, impact, and interactions of all reported parameters for the FOCR for the first time in its 175 year long history. We showed that hydroxide was the most active catalyst leading to an oxalate yield of up to 93%. The addition of water, silica, and carbon has a poisonous effect on the reaction and reduced the oxalate yield to 22, 15, and 29%, respectively. In CO_2 no oxalate was formed, and in CO atmosphere, the reaction was largely suppressed leading to a 35% oxalate yield. Conversely, nitrogen, argon, and hydrogen are the most suitable atmospheres, allowing oxalate yields of up to 93%, and purging of the reaction increased the oxalate yield up to 35%.

In a nitrogen atmosphere, the temperature has the highest influence followed by reaction time and purging. In the hydrogen atmosphere reaction time and temperature both have large equal influences. Catalyst loading showed no influence on conversion or selectivity in either atmosphere. Therefore, even lower catalyst loadings below the previously proposed 2 wt % KOH could be used in the future. We did not find any indication for the decomposition of formate to carbonate as suggested for temperatures below 380 °C or any involvement of hydroxide in carbonate formation. We conclude that the overall behavior indicates a predominantly linear reaction cascade starting with the formate to oxalate reaction. This is followed by oxalate decomposition to carbonate and then the loss of carbon from the obtained solids as either nonsoluble elemental or gaseous carbon. These results help to identify optimal reaction conditions for new FOCR reactors, contribute to the ongoing mechanistic discussions, and develop new reactor concepts.

ASSOCIATED CONTENT

SI **Supporting Information**

The Supporting Information is available free of charge at https://pubs.acs.org/doi/10.1021/acssuschemeng.1c04539.

Experimental methods; analysis of categorical and numerical factors; response surface model 1 with nitrogen as atmosphere; response surface model 2 with hydrogen as atmosphere (PDF)

AUTHOR INFORMATION

Corresponding Author

Gert-Jan M. Gruter − *Van 't Hoff Institute for Molecular Sciences, University of Amsterdam, 1090 GD Amsterdam, The Netherlands; Avantium Chemicals BV, 1014 BV Amsterdam, The Netherlands;* ● orcid.org/0000-0003-4213-0025; Email: g.j.m.gruter@uva.nl

Authors

Eric Schuler − *Van 't Hoff Institute for Molecular Sciences, University of Amsterdam, 1090 GD Amsterdam, The Netherlands*

Marit Stoop − *Van 't Hoff Institute for Molecular Sciences, University of Amsterdam, 1090 GD Amsterdam, The Netherlands*

N. Raveendran Shiju − *Van 't Hoff Institute for Molecular Sciences, University of Amsterdam, 1090 GD Amsterdam, The Netherlands;* ● orcid.org/0000-0001-7943-5864

Complete contact information is available at:
https://pubs.acs.org/10.1021/acssuschemeng.1c04539

Notes

The authors declare no competing financial interest.

ACKNOWLEDGMENTS

REFERENCES

(1) Jullion; Crane; MacDougall; Rawson. Ueber Die Fabrication von Kleesäure. *Polytech. J.* **1852**, *124* (42), 175−181.

(2) Laber, G. Oxalsäure. In *Ullmanns Enzyklopädie der technischen Chemie*; Wiley-VCH Verlag GmbH & Co. KGaA: Weinheim, 1962; Vol. *13*, pp 51−55.

(3) Florio, P. A. Oxalic Acid. In *Kirk-Othmer Encyclopedia of Chemical Technology*, 2nd ed.; Interscience Publishers: 1967; Vol. *14*, pp 356−373.

(4) Dance, T. Assessment and Geological Characterisation of the CO2CRC Otway Project CO2 Storage Demonstration Site: From Prefeasibility to Injection. *Mar. Pet. Geol.* **2013**, *46*, 251−269.

(5) Ouellet, A.; Bérard, T.; Desroches, J.; Frykman, P.; Welsh, P.; Minton, J.; Pamukcu, Y.; Hurter, S.; Schmidt-Hattenberger, C. Reservoir Geomechanics for Assessing Containment in CO2 Storage: A Case Study at Ketzin, Germany. *Energy Procedia* **2011**, *4*, 3298−3305.

(6) Al-Mamoori, A.; Krishnamurthy, A.; Rownaghi, A. A.; Rezaei, F. Carbon Capture and Utilization Update. *Energy Technol.* **2017**, *5*, 834−849.

(7) Raza, A.; Gholami, R.; Rezaee, R.; Rasouli, V.; Rabiei, M. Significant Aspects of Carbon Capture and Storage − A Review. *Petroleum* **2019**, *5* (4), 335−340.

(8) Anwar, M. N.; Fayyaz, A.; Sohail, N. F.; Khokhar, M. F.; Baqar, M.; Yasar, A.; Rasool, K.; Nazir, A.; Raja, M. U. F.; Rehan, M.; et al. CO2 Utilization: Turning Greenhouse Gas into Fuels and Valuable Products. *J. Environ. Manage.* **2020**, *260*, 110059.

(9) Meylan, F. D.; Moreau, V.; Erkman, S. CO2 Utilization in the Perspective of Industrial Ecology, an Overview. *J. CO2 Util.* **2015**, *12*, 101−108.

(10) Cuéllar-Franca, R. M.; Azapagic, A. Carbon Capture, Storage and Utilisation Technologies: A Critical Analysis and Comparison of Their Life Cycle Environmental Impacts. *J. CO2 Util.* **2015**, *9*, 82−102.

(11) Artz, J.; Müller, T. E.; Thenert, K.; Kleinekorte, J.; Meys, R.; Sternberg, A.; Bardow, A.; Leitner, W. Sustainable Conversion of Carbon Dioxide: An Integrated Review of Catalysis and Life Cycle Assessment. *Chem. Rev.* **2018**, *118* (2), 434−504.

(12) Ronda-Lloret, M.; Yang, L.; Hammerton, M.; Marakatti, V. S.; Tromp, M.; Sofer, Z.; Sepúlveda-Escribano, A.; Ramos-Fernandez, E. V.; Delgado, J. J.; Rothenberg, G.; et al. Molybdenum Oxide Supported on Ti3AlC2 Is an Active Reverse Water-Gas Shift Catalyst. *ACS Sustainable Chem. Eng.* **2021**, *9* (14), 4957−4966.

(13) Bollen, J. Role of Carbon Capture and Storage (CCS) or Use (CCU) on Climate Mitigation. In *Designing Sustainable Technologies, Products and Policies*; Springer International Publishing: Cham, Switzerland, 2018; pp 307−309. DOI: 10.1007/978-3-319-66981-6_33.

(14) *Carbon Dioxide as Chemical Feedstock*; Aresta, M., Ed.;Wiley-VCH Verlag GmbH & Co. KGaA: 2010. DOI: 10.1002/9783527629916.

(15) *Carbon Dioxide Utilisation*; Styring, P., Quadrelli, E. A., Armstrong, K., Eds.; Elsevier: 2015. DOI: 10.1016/C2012-0-02814-1.

(16) Gnanakumar, E. S.; Chandran, N.; Kozhevnikov, I. V.; Grau-Atienza, A.; Ramos Fernández, E. V.; Sepulveda-Escribano, A.; Shiju, N. R. Highly Efficient Nickel-Niobia Composite Catalysts for Hydrogenation of CO2 to Methane. *Chem. Eng. Sci.* **2019**, *194*, 2−9.

(17) Ronda-Lloret, M.; Rothenberg, G.; Shiju, N. R. A Critical Look at Direct Catalytic Hydrogenation of Carbon Dioxide to Olefins. *ChemSusChem* **2019**, *12* (17), 3896−3914.

(18) Devid, E. J.; Ronda-Lloret, M.; Zhang, D.; Schuler, E.; Wang, D.; Liang, C.-H.; Huang, Q.; Rothenberg, G.; Shiju, N. R.; Kleyn, A. W. Enhancing CO 2 Plasma Conversion Using Metal Grid Catalysts. *J. Appl. Phys.* **2021**, *129* (5), 053306.

(19) Ronda-Lloret, M.; Marakatti, V. S.; Sloof, W. G.; Delgado, J. J.; Sepúlveda-Escribano, A.; Ramos-Fernandez, E. V.; Rothenberg, G.; Shiju, N. R. Butane Dry Reforming Catalyzed by Cobalt Oxide Supported on Ti2AlC MAX Phase. *ChemSusChem* **2020**, *13* (23), 6401−6408.

(20) Ronda-Lloret, M.; Wang, Y.; Oulego, P.; Rothenberg, G.; Tu, X.; Shiju, N. R. CO2Hydrogenation at Atmospheric Pressure and Low Temperature Using Plasma-Enhanced Catalysis over Supported Cobalt Oxide Catalysts. *ACS Sustainable Chem. Eng.* **2020**, *8* (47), 17397−17407.

(21) *Oxalic acid from CO2 using Electrochemistry At demonstratioN scale\OCEAN Project*; H2020. CORDIS, European Commission. https://cordis.europa.eu/project/id/767798 (accessed 2020-02-04).

(22) Jin, F.; Gao, Y.; Jin, Y.; Zhang, Y.; Cao, J.; Wei, Z.; Smith, R. L. High-Yield Reduction of Carbon Dioxide into Formic Acid by Zero-Valent Metal/Metal Oxide Redox Cycles. *Energy Environ. Sci.* **2011**, *4* (3), 881−884.

(23) Zhong, H.; Wang, L.; Yang, Y.; He, R.; Jing, Z.; Jin, F. Ni and Zn/ZnO Synergistically Catalyzed Reduction of Bicarbonate into Formate with Water Splitting. *ACS Appl. Mater. Interfaces* **2019**, *11* (45), 42149−42155.

(24) Jouny, M.; Luc, W.; Jiao, F. General Techno-Economic Analysis of CO 2 Electrolysis Systems. *Ind. Eng. Chem. Res.* **2018**, *57* (6), 2165−2177.

(25) Aldaco, R.; Butnar, I.; Margallo, M.; Laso, J.; Rumayor, M.; Dominguez-Ramos, A.; Irabien, A.; Dodds, P. E. Bringing Value to the Chemical Industry from Capture, Storage and Use of CO2: A Dynamic LCA of Formic Acid Production. *Sci. Total Environ.* **2019**, *663*, 738−753.

(26) Murcia Valderrama, M. A.; van Putten, R.-J.; Gruter, G.-J. M. The Potential of Oxalic − and Glycolic Acid Based Polyesters (Review). Towards CO2 as a Feedstock (Carbon Capture and Utilization − CCU). *Eur. Polym. J.* **2019**, *119*, 445−468.

(27) Murcia Valderrama, M. A.; van Putten, R.-J.; Gruter, G.-J. M. PLGA Barrier Materials from CO 2. The Influence of Lactide Co-Monomer on Glycolic Acid Polyesters. *ACS Appl. Polym. Mater.* **2020**, *2* (7), 2706−2718.

(28) Wang, B.; Gruter, G. J. M. Polyester Copolymer. WO2018211132A1, 2017.

(29) Wang, B.; Gruter, G. J. M. Polyester Copolymer. WO2018211133A1, 2017.

(30) Schuler, E.; Demetriou, M.; Shiju, N. R.; Gruter, G.-J. M. Towards Sustainable Oxalic Acid from CO2 and Biomass. *ChemSusChem* **2021**, *14*, 3636.

(31) Goldschmidt, M. Process of Making Oxalates. US659733A, October 16, 1900.

(32) Wiens, A. Process of Making Oxalates. US714347, November 25, 1902.

(33) Strauss, D. Manufacture of Oxalates. US1038985, September 17, 1912.

(34) Mewburn, E. Manufacture of Oxalates and Oxalic Acid. GB160747, January 6, 1922.

(35) Paulus, H. W. Method of Converting Formate into Oxalates. US1445163, 1923.

(36) Wallace, W. Producing Oxalates from Formates. US1506872, September 2, 1924.

(37) Bredt Otto, P. C. Treatment of Formates of Metals of the Alkali-Earth Group. US1622991, 1927.

(38) Enderli, M. Process for the Production of Caustic Potash and Oxalic Acid. US2002342, May 21, 1935.

(39) Hene, E. Process for Making Potassium Oxalate. US2004867, June 11, 1935.

(40) Enderli, M.; Schrodt, A. Process for the Preparation of Potassium Oxalate from Potassium Formate. US2033097, March 3, 1936.

(41) Freidlin, L. K. Volumetric Determination of Alkali Metal Carbonates and Oxalates in Mixture with Formates in *Scientific reports of Moscow University*, **1936**, 152−156.

(42) Freidlin, L. K. On the Production of Oxalic Acid in the USSR. *Ind. Org. Chem. (Prom-st. Org. Khim.)* **1937**, *3*, 681−686.

(43) Freidlin, L. K.; Balandin, A. A.; Lebedeva, A. I. Thermal Decomposition of Lithium Formate. *Russ. Chem. Bull. (Izv. Akad. Nauk SSSR, Ser. Khim.)* **1941**, *2*, 261−267.

(44) Freidlin, L. K.; Balandin, A. A.; Lebedeva, A. I. On the Consecutive Stages of the Thermal Conversion of Formates into Oxalates. *Russ. Chem. Bull. (Izv. Akad. Nauk SSSR, Ser. Khim.)* **1941**, *2*, 275−288.

(45) Freidlin, L. K. Thermal Transformation of Potassium and Sodium Formates in Presence of Alkali Hydroxides. *Zh. Prikl. Khim.* **1937**, *10* (6), 1086−1094.

(46) Freidlin, L. K. Kinetics of Potassium Formate Decomposition in Presence of Alkali Metals. *Zh. Obs. Khim.* **1937**, *7* (11), 1675−1683.

(47) Freidlin, L. K. Selectiive Effect of Different Caltalysts on Converting Fusible Formates to Oxalates. *Zh. Prikl. Khim.* **1938**, *11* (6), 975−980.

(48) Freidlin, L. K. Kinetics of Sodium Formate Thermal Decomposition. *Trans. All-Union Acad. Food Ind. named after Stalin* **1939**, No. 10, 145−157.

(49) Freidlin, L. K.; Balandin, A. A.; Lebedeva, A. I. Thermal Decomposition of Tallium Formate. *Bull. Acad. Sci. URSS, Cl. Sci. Math. Nat., Ser. Chem.* **1940**, *6*, 955−962.

(50) Freidlin, L. K.; Balandin, A. A.; Lebedeva, A. I. On the Capacity of Metal Formates to Be Transformed into Oxalates. *Russ. Chem. Bull. (Izv. Akad. Nauk SSSR)* **1941**, *2*, 268−274.

(51) Freidlin, L. K.; Balandin, A. A.; Lebedeva, A. I. Thermal Decomposition of Caesium Formate. *Russ. Chem. Bull. (Izv. Akad. Nauk SSSR)* **1941**, *2*, 255−262.

(52) Freidlin, L. K.; Balandin, A. A.; Lebedeva, A. I. Thermal Decomposition of Rubidium Formate. *Russ. Chem. Bull. (Izv. Akad. Nauk SSSR)* **1941**, *2*, 247−256.

(53) Górski, A.; Kraśnicka, A. D. Influence of the Cation on the Formation of Free Hydrogen and Formaldehyde in the Thermal Decomposition of Formates. *J. Therm. Anal.* **1987**, *32* (5), 1345−1354.

(54) Górski, A.; Kraśnicka, A. D. Origin of Organic Gaseous Products Formed in the Thermal Decomposition of Formates. *J. Therm. Anal.* **1987**, *32* (4), 1243−1251.

(55) Górski, A.; Kraśnicka, A. D. The Importance of the CO 2 2− Anion in the Mechanism of Thermal Decomposition of Oxalates. *J. Therm. Anal.* **1987**, *32* (4), 1229−1241.

(56) Górski, A.; Kraśnicka, A. D. Formation of Oxalates and Carbonates in the Thermal Decompositions of Alkali Metal Formates. *J. Therm. Anal.* **1987**, *32* (6), 1895−1904.

(57) Shishido, S.; Masuda, Y. The Gaseous Products Formed in the Thermal Decompositions of Formates. *Nippon Kagaku Kaishi* **1973**, 185−188.

(58) Shishido, S.; Masuda, Y. Thermal Decomposition of Alkali Metal Formates. *Nippon Kagaku Kaishi* **1976**, *1*, 66−70.

(59) Li, A.; Li, Y. Method and Equipment for Producing Sodium Oxalate by Spray Dehydrogenation of Sodium Formate. CN1948260A, April 18, 2007.

(60) Cao, Z.; Cao, Y. Production of Oxalates, Oxalic Acid and Dihydrogen Phosphate Salt by Dehydrogenation of Formate Salts. CN101462943A, June 24, 2009.

(61) Li, Y.; Ma, Q.; Li, A.; Li, F.; Liu, C.; Li, Q. Process and Equipment of Continuous Dehydrogenating Producing Sodium Oxalate by Circulating Fluidized Bed. CN200710004103, 2010.

(62) Li, A.; Li, Y.; Zhao, Z.; Zhang, A.; Li, Z. Technology of Producing Sodium Oxalate by Continuous Dehydrogenation of Sodium Formate and Its Equipment. CN1903821B, January 31, 2012.

(63) Kaczur, J. J.; Lakkaraju, P. P.; Parajuli, R. R. Process for Producing Oxalic Acid. WO2017121887A1, July 20, 2017.

(64) Lakkaraju, P. S.; Askerka, M.; Beyer, H.; Ryan, C. T.; Dobbins, T.; Bennett, C.; Kaczur, J. J.; Batista, V. S. Formate to Oxalate: A Crucial Step for the Conversion of Carbon Dioxide into Multi-Carbon Compounds. *ChemCatChem* **2016**, *8* (22), 3453−3457.

(65) Schuler, E.; Ermolich, P. A.; Shiju, N. R.; Gruter, G. M. Monomers from CO 2 : Superbases as Catalysts for Formate-to-Oxalate Coupling. *ChemSusChem* **2021**, *14* (6), 1517−1523.

(66) Xie, K. Microwave Dehydrogenation Process for Preparing Sodium Oxalate. CN1727322A, February 1, 2006.

(67) Hartman, K.; Hisatsune, I. C. The Kinetics of Formate Ion Pyrolysis in Alkali Halide Matrices. *J. Phys. Chem.* **1966**, *70*, 1281−1287.

(68) Ovenall, D. W.; Whiffen, D. H. Electron Spin Resonance and Structure of the Co-2 Radical Ion. *Mol. Phys.* **1961**, *4* (2), 135−144.

(69) Schuler, E.; Morana, M.; Ermolich, P. A.; Shiju, N. R.; Gruter, G.-J. M. Perspective: Formate as a Key Intermediate in CCU. *Green Chem.* **2021**.

(70) Myers, W. Response Surface Methodology. In *Encyclopedia of Biopharmaceutical Statistics*, 3rd ed.; CRC Press: 2012; pp 1171−1179.

(71) Schuler, E.; Perez de Alba Ortiz, A.; Ensing, B.; Shiju, N. R.; Gruter, G.-J. M. Understanding a Key Step in CO2 to Polymers: The Role of Alkali Hydroxides in Formate Coupling Reactions. *ACS Catal.* **2021**.

(72) Myers, R. H.; Montgomery, D. C.; Anderson-Cook, C. M. *Response Surface Methodology: Process and Product Optimization Using Designed Experiments*, 4th ed.; John Wiley & Sons Inc.: 2016.

(73) Koter, S. Ion-Exchange Membranes for Electrodialysis A Patents Review. *Recent Pat. Chem. Eng.* **2011**, *4* (2), 141−160.

(74) Novalic, S.; Kongbangkerd, T.; Kulbe, K. D. Recovery of Organic Acids with High Molecular Weight Using a Combined Electrodialytic Process. *J. Membr. Sci.* **2000**, *166* (1), 99−104.

(75) Ferrer, J. S. J.; Laborie, S.; Durand, G.; Rakib, M. Formic Acid Regeneration by Electromembrane Processes. *J. Membr. Sci.* **2006**, *280* (1−2), 509−516.

(76) Trivedi, G. S.; Shah, B. G.; Adhikary, S. K.; Indusekhar, V. K.; Rangarajan, R. Studies on Bipolar Membranes. Part II — Conversion of Sodium Acetate to Acetic Acid and Sodium Hydroxide. *React. Funct. Polym.* **1997**, *32* (2), 209−215.

(77) Li, H.; Mustacchi, R.; Knowles, C. J.; Skibar, W.; Sunderland, G.; Dalrymple, I.; Jackman, S. A. An Electrokinetic Bioreactor: Using Direct Electric Current for Enhanced Lactic Acid Fermentation and Product Recovery. *Tetrahedron* **2004**, *60* (3), 655−661.

(78) Strathmann, H. Preparation and Characterization of Ion-Exchange Membranes. In *Ion-Exchange Membrane Separation Processes*; Membrane Science and Technology 9; Elsevier: Amsterdam, 2004; pp 89−146..